JOURNAL OF MATERIALS SCIENCE 25 (1990) 69–75

Characterization of carbon-filled polymers by small-angle scattering techniques

G. D. WIGNALL
Solid State Division, Oak Ridge National Laboratory Oak Ridge, Tennessee 37831-6031, USA
N. R. FARRAR, S. MORRIS
Raychem Corporation, Menlo Park, California, USA

Both small-angle X-ray and neutron scattering (SAXS and SANS) have been used to characterize a series of carbon black-filled polyethylene composities. High-resolution methods were used to evaluate particle sizes and aggregation in the size range 10 to 80 nm. The SANS data give an excellent fit to a two-correlation function model over the whole concentration range, both in the shape and absolute magnitude of the scattering. Comparison of SAXS and SANS data indicates the presence of a third phase, most probably voids at the surface of the carbon particles. Because the voids have virtually no neutron contrast with the polyethylene matrix, a two-phase model may be employed for analysis of the SANS data, which gives an accurate description of the morphology and surface characteristics of the carbon particles.

1. Introduction

Carbon black is extensively used to modify the mechanical and electrical properties of polymers and elastomers. The size and distribution of the individual particles and agglomerates have an important effect on properties. Agglomeration of the particles into larger aggregates is known to occur in highly loaded polymers, and can significantly affect the strength and electrical resistivity. Agglomerates are difficult to detect or characterize, particularly for opaque carbon black–polymer composites which are not amenable to optical methods. Electron microscopy has been used extensively to study the state of dispersion of carbon black particles [1–4], though only thin microtomed sections can be examined and it is difficult to produce results characteristic of the bulk materials without averaging large numbers of repeated measurements.

Small-angle X-ray scattering (SAXS) has the advantage that bulk samples (thickness $\simeq$ 0.1 cm) may be examined without sectioning, and the results give an average over statistically large numbers of particles. This technique has been applied to the characterization of silica [5–7] and carbon black [7] particles in polymers and rubbers. SAXS techniques are generally applied to study structures in the size range 1 to 100 nm by measuring the intensity of scattering $I(Q)$ as a function of Q where

$$Q = \frac{4\pi}{\lambda} \sin \theta \qquad (1)$$

λ is the incident wavelength and 2θ is the angle of scatter. Ideally the incident radiation is monochromatic and the experiment uses a point source, sample and detector. In this case there would be no distortion or smearing of the scattering pattern. In practice, in order to achieve a measurable intensity, a finite source, sample and detector are used so that the measured pattern is averaged over a range of wavelengths and angles.

Previous experiments [5–7] showed that SAXS was a promising method to study structures in the size range 20 to 40 nm. In this work we have applied small-angle scattering to study polymer composites consisting of carbon black dispersed in high-density polyethylene. At high filler loadings, conductivity arises as a result of the tunnelling between adjacent carbon particles. The conductivity depends very much on particle separation, which in turn depends upon temperature. The separation becomes larger as the temperature is raised, causing a decrease in conductivity. Systems can be designed to yield a large change in particle separation with temperature and a so-called anomalous positive temperature coefficient of resistivity is observed. This effect is the basis of the use of such materials as control devices. One widely used application is as a self-regulating heater whose power decreases as the temperature rises and cuts off completely at a predesigned temperature. Such devices have also been designed as reusable fuses. It is especially difficult to study the effect of changes in structure on electrical properties because the electrical properties are highly sensitive to a combination of structural and materials parameters. The aim of this study was to evaluate SAXS as a nondestructive technique for eliminating material parameters and allowing a quantitative correlation of structure with properties.

Preliminary experiments [8] indicated that the

*Present address: Hewlett Packard Laboratories, Palo Alto, California, USA.

0022–2461/90 $03.00 + .12

dimensions of the agglomerates in this type of system exceeded 40 nm and for this reason high-resolution instrumentation was employed for SAXS measurements [9]. Previous studies [5–7] utilized nickel-filtered CuKα radiation in conjunction with slit collimation, though the finite range of angles ($\Delta\theta$) accepted by the detector introduces instrumental smearing effects which distort the measured diffraction pattern. The data were either desmeared using numerical correction procedures [7] or analysed via theoretical approaches which included instrumental smearing [5]. For example, in the latter case, a Q^{-4} variation in the Porod regime is changed to Q^{-3} in the long slit camera. No account was taken of smearing of the measured data due to the wavelength spread of the incident beam ($\Delta\lambda$), though β-filtered radiation produces measurable distortion of the diffraction pattern, particularly at small angles [10]. In view of the large dimensions of the aggregates in the composites studied, it is important to use high-resolution techniques and the present study utilized a 10 m SAXS camera with point geometry and a crystal monochromator which minimizes smearing effects on the measured pattern by restricting $\Delta\theta$ and $\Delta\lambda$ [10, 11]. Even higher resolution can be obtained using the 30 m small-angle neutron scattering camera [12] at Oak Ridge National Laboratory (ORNL). This facility provides complementary structural data and has been carefully evaluated for resolution effects [11]. It will be seen in subsequent sections that the Porod [13, 14] and Debye–Bueche [15] analyses used previously [5–7] do not give a complete description of the observed scattering patterns of carbon–polyethylene composites. A refinement of the theory developed by Debye *et al.* [16] was shown to fit the data over a wide range of composition and Q and gave information on the long-range structure of the composites. In addition, methods based on fractal concepts [17] were used to examine the surface characteristics of the carbon particles.

2. Experimental details

The scattering data were taken on the facilities of the National Center for Small-Angle Scattering Research (NCSASR) at ORNL. The neutron measurements were performed on the NCSASR 30 m SANS instrument [12]. The incident beam of wavelength 0.475 nm ($\Delta\lambda/\lambda = 6\%$) was collimated by source and sample slits separated by a distance of 7.5 m. The area detector ($64 \times 64\,cm^2$), with $1\,cm^2$ element size mounted on rails inside a 20 m vacuum flight path, was positioned at a distance of 18.9 m from the sample to give an effective Q range of $0.03 < Q < 0.3\ nm^{-1}$. In addition, several samples were examined with a sample–detector distance of 10 m which extends the maximum Q to $0.55\,nm^{-1}$. In all Q ranges, the scattering patterns were corrected on a cell by cell basis for instrumental backgrounds and detector efficiency variation, divided by the sample transmission (T) and thickness (t), and normalized to a constant incident flux. Correction for the spatial variation of detector efficiency was accomplished by dividing all measured scattering patterns by the background corrected scattering from an isotropic scatterer (H_2O). All the scattering patterns studied exhibited azimuthal symmetry and were radially averaged. The intensity data, $I(Q)$, were converted to an absolute differential scattering cross section $d\Sigma/d\Omega$ per unit sample volume (in units of cm^{-1}) by means of precalibrated secondary standards [18].

The SAXS measurements were performed on the ORNL 10 m SAXS facility [9]. The incident wavelength of 0.154 nm was taken from a 12 kW rotating anode source (Rigaku–Denki) with a copper target, where the K_β radiation was removed by reflection from a pyrolytic graphite monochromator. Collimation was achieved with a circular 1 mm diameter aperture at the source and a 1 mm × 1 mm square aperture 1.6 m from the source. The sample was placed at a distance of 3.1 m from the entrance aperture with a 2.2 mm diameter guard slit to reduce parasitic scattering. The sample-to-detector distance was 5.1 m, giving an effective Q range of 0.025 to $1\,nm^{-1}$. The detector was a 20 cm × 20 cm position-sensitive proportional counter filled with xenon gas and quenched with CO_2. This geometry approximates to pinhole collimation very well. Data were normalized to the incident X-ray flux with a monitoring scintillation counter located just down-stream from the graphite monochromator and source slit. Variations in detection efficiency over the area of the detector were corrected by use of a ^{55}Fe source ($\sim 10\,\mu Ci$) placed at the sample position. In this source, transmutation of ^{55}Mn occurs by β emission and an immediate capture, the electron producing a strong isotropic Mn$K\alpha$ fluorescence. As with the SANS experiments, all patterns were divided by the product, tT, and corrected on a cell by cell basis for instrumental backgrounds, detector efficiency, normalized to constant incident flux, and converted to an absolute differential X-ray scattering cross-section $d\Sigma/d\Omega$ by comparison with precalibrated secondary standards [19].

3. Materials preparation and physical properties

Samples were prepared using XC-72 carbon black supplied by Cabot Corporation and Marlex 6003 high-density polyethylene. This combination of filler and matrix was selected as being typical of filled polymers designed to have good mechanical properties with a low electrical resistivity at moderate loadings. Data on XC-72, supplied by the manufacturer is given in Table I. The density of the polyethylene component was measured experimentally by weighing in air and water. A value of $0.962\,g\,cm^{-3}$ was recorded. The carbon black was dried for 12 h at 200° C before mixing with the high-density polyethylene in a Brabender mixer. The resin pellets were melted for

TABLE I Properties XC-72

Surface area			Particle size (nm)
N_2 adsorption ($m^2\,g^{-1}$)	Iodine adsorption ($m^2\,g^{-1}$)	DBP adsorption $cm^3/100g$	
254	192	184	30

1 min and the filler incorporated over a maximum mixing time of 5 mins. The Brabender temperature was 190° C and the mixing speed was 60 r.p.m.

Samples were then moulded into approximately 1 mm thick slabs at 182° C for 2 min. All samples contained 1% by weight of an antioxidant to prevent polymer degradation during processing. The density of the antioxidant is quoted as 1.05 g cm^{-3}. The weight fraction of carbon black was estimated from sample weighings. Density and volume fraction estimates shown in Table II are based on these values. The antioxidant was taken into account in these calculations.

Density was also measured experimentally by weighing samples in air and water. Weight fraction was also checked by thermogravimetric analysis. Results are quoted in Table II; however, these are not considered as accurate as estimates based on weighing the individual components. In-plane and normal electrical resistivity was also measured using a four-point probe technique. Precise measurements could only be made for samples containing > 21 wt% carbon black.

4. Scattering Theory

The Debye–Bueche formula [15, 20] is given by

$$\frac{d\Sigma}{d\Omega}(Q) = \frac{d\Sigma}{d\Omega}(0)\frac{1}{(1 + Q^2a^2)^2} \quad (2)$$

where a is a correlation length defined in the correlation function

$$\gamma(r) = \exp(-r/a) \quad (3)$$

which describes the scattering fluctuations in the material. Equation 3 applies to a random interpenetrating two-phase system and describes the correlation distance of the short range fluctuations in scattering power. Equation 2 has been widely used to measure domain dimensions in porous materials [21] and two-phase blends [20, 22].

For other systems [16, 23] the exponential approximation for the correlation function has been extended to include a Gaussian [16, 23] term

$$\gamma(r) = f\exp(-r/a_1) + (1 - f)\exp(-r/a_2)^2 \quad (4)$$

where f is a fractional contribution factor for the two components of the correlation function. The two correlation lengths a_1 and a_2 represent the short-range and long-range fluctuations in scattering power, respectively. Other types of correlation functions have been discussed by Yuen and Kissinger [24], in a study of light scattering from polymer blends, though it was concluded that the inhomogeneities were best described by Equation [4]. For this correlation function the coherent SANS cross-section is given by

$$\frac{d\Sigma}{d\Omega} = (\varrho_1 - \varrho_2)^2\phi(1 - \phi)4\pi \times \left[\frac{2fa_1^3}{(1 + Q^2a^2)^2} + \frac{(1 - f)\pi^{1/2}a_2^3}{4}\exp\left(\frac{-Q^2a_2^2}{4}\right)\right] \quad (5)$$

where ϱ_1 and ϱ_2 are the scattering length densities of the two phases and ϕ is the volume fraction of one phase. Equation 5 does not include the scattering from the polyethylene matrix and antioxidant. Because of the cancellation between the scattering lengths of carbon ($b_C = 0.665 \times 10^{-12}$ cm) and hydrogen ($b_H = -0.374 \times 10^{-12}$ cm) there is virtually no coherent signal from polyethylene and the background signal is mainly incoherent, arising largely from H^1 nucleii. This forms a constant background $\sim 1\,cm^{-1}$ which is independent of Q and was subtracted from all scattering patterns and constitutes a very minor correction to the strong coherent scattering for all blends ($d\Sigma/d\Omega \sim 10^3$ to $10^5\,cm^{-1}$ at $Q = 0$). The coherent SAXS cross-section may also be obtained from Equation 5 by substituting the electron density times the Thompson scattering factor (0.282×10^{-12} cm) for the scattering length density [19].

5. Results and discussion

Figure 1 shows a conventional Guinier plot of the coherent SANS cross-section from a blend of 0.53 vol % carbon black in high-density polyethylene (Marlex). The plot is highly nonlinear, indicating that the Guinier analysis is inapplicable, presumably due to the large polydispersity of particle sizes in the disperse phase. Figure 2 shows a typical Debye–Bueche plot of the data in Fig. 1. For $f = 1$ in Equations 4 and 5, a plot of $(d\Sigma/d\Omega)^{-1/2}$ against Q^2 should be linear, and it may be seen that this is a much better approximation than the Guinier model. However, the data deviates from straight-line behaviour at higher Q and the deviations are more pronounced when plotted over a

TABLE II

Sample number	Carbon weight fraction calculated (%)	Carbon volume fraction calculated (%)	S.G. calculated (g cm^{-3})	S.G. measured (g cm^{-3})	Carbon weight fraction TGA (%)	Electrical resistivity	
						In plane (Ω cm)	Normal (Ω cm)
1	60	44.5					
2	55	39.5					
3	50	34.8	1.256	1.254	49.8	140	70
4	40	26.3	1.184	1.181	40.1	350	350
5	27	16.5	1.100	1.070	22.8	13 000	400
6	21	12.4	1.065	1.036	16.3	> 1000 meg	> 1000 meg
7	10	5.6	1.010	1.004	9.8	> 1000 meg	> 1000 meg
8	2	1.08	0.973	0.962	2.7	> 1000 meg	> 1000 meg
9	1	0.53	0.968	0.960	1.5	> 1000 meg	> 1000 meg
10	0.5	0.27	0.966	0.963	1.0	> 1000 meg	> 1000 meg

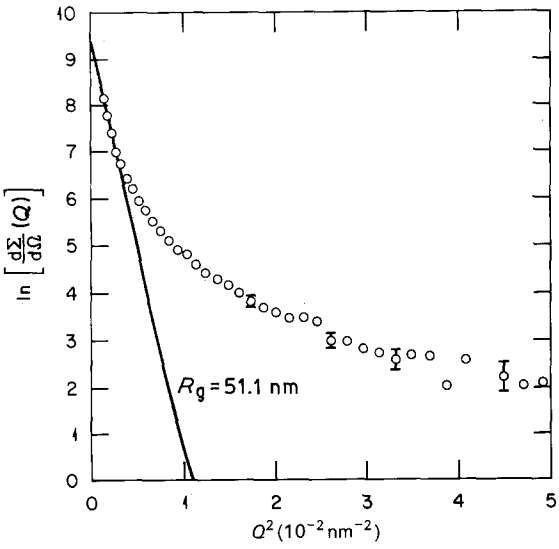

Figure 1 Guinier plot for 0.53 vol % carbon black in polyethylene.

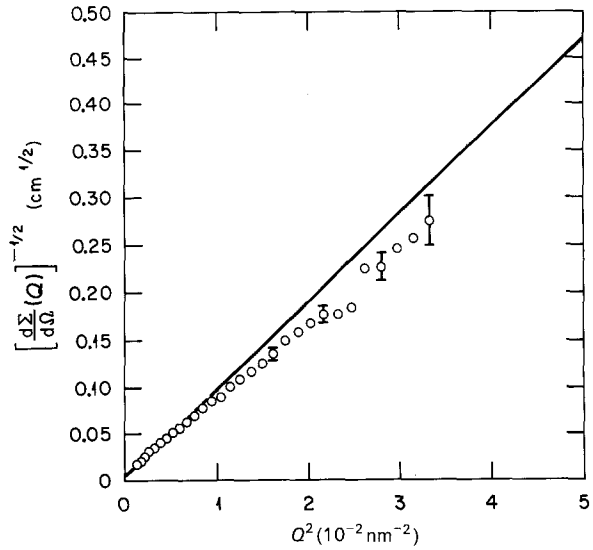

Figure 2 Debye–Bueche plot for 0.53 vol % carbon black in polyethylene.

wider Q-range. Figure 3 shows a plot of the SANS data from a sample with 34.8 vol % carbon black compared to the two-correlation function Debye theory (Equations 4 and 5) with the fitting parameters

$$A_1 = 8\pi a_1^3 f\phi(1-\phi)(\varrho_1-\varrho_2)^2 \quad (6)$$

and

$$A_2 = \pi^{3/2}a_2^3(1-f)\phi(1-\phi)(\varrho_1-\varrho_2)^2 \quad (7)$$

It may be seen that this model gives an excellent fit to the SANS data for this composition and similar fits result over the whole composition range. The SAXS data also give reasonable fits to this model though the parameters (a_1, a_2, etc.) are different for SAXS and SANS as discussed below.

Table III shows the fitting parameters (a_1, a_2, A_1, A_2) for the SANS data as a function of the volume fraction of carbon black (ϕ). Also shown are the fractional contribution factor (f), the specific surface (S), the distance of heterogeneity (l_c) and the volume of heterogeneity $\bar{V}$, which may be derived [23] from the fitting parameters as follows

$$f = [1 + (8/\pi^{1/2})(a_1/a_2)^3]^{-1} \quad (8)$$

$$A = \frac{A_2}{A_1} = [(1-f)\pi^{1/2}a_2^3]/8fa_1^3 \quad (9)$$

$$f/a_1 = S/[4\phi(1-\phi)] \quad (10)$$

$$\bar{l}_c/2 = fa_1 + 2(1-f)a_2\pi^{1/2} \quad (11)$$

$$V = 4[2fa_1^3 + (1-f)\pi^{1/2}a_2^3/r] \quad (12)$$

The contribution $(1-f)$ of the long-range correlation function is largest for small loadings of carbon black and decreases progressively as ϕ increases and the distribution of particles becomes more uniform. This trend is mirrored in the behaviour of the distance (l_c) and volume ($\bar{V}$) of heterogeneity, which are largest for small ϕ and decrease progressively for high loadings of carbon black. The specific surface (S) is approximately proportional to ϕ up to a loading of 16.5 vol %. For high loadings, S increases faster than ϕ (Fig. 4). Table IV shows a comparison of the absolute cross-sections at $Q = 0$ compared to the values calculated from the model.

$$\frac{d\Sigma}{d\Omega}(0) = A_1 + A_2 \quad (13)$$

Such comparisons are not possible unless the data are taken in absolute units and provide a stringent test for the analysis which must reproduce not only the shape, but also the absolute magnitude of the scattering. The discrepancies for any individual concentration are in the range $\mp 30\%$, though there is no systematic distortion and the deviations are both positive and negative. Such agreement is very good in view of the uncertainty associated with calibration and the extreme sensitivity

TABLE III SANS fitting parameters for carbon black–polyethylene blends

ϕ (vol %)	a_1 (nm)	A_1 (10^3 cm^{-1})	a_2 (nm)	A_2 (10^3 cm^{-1})	f	s (μ^{-1})	$\bar{l}_c$ (nm)	$\bar{V}$ (10^{-3} nm^3)
45.5	12.7	65.5	55.5	32.2	0.970	75.4	27.6	25.0
39.9	14.7	99.7	64.0	59.6	0.968	62.9	32.0	39.5
34.8	17.8	132.0	60.9	44.9	0.962	48.9	38.4	58.6
26.3	19.5	162.8	66.4	77.5	0.950	37.7	43.0	82.3
16.5	28.8	258.9	74.3	58.7	0.943	18.0	61.8	222
12.4	29.0	171.8	77.5	75.6	0.905	13.5	66.5	254
5.6	29.7	120.5	79.5	56.3	0.901	6.4	67.4	297
1.08	31.5	28.1	86.4	21.0	0.859	1.17	75.7	410
0.53	30.9	12.9	84.3	10.9	0.835	0.56	76.2	411
0.27	28.9	5.3	80.8	4.1	0.820	0.30	73.1	361

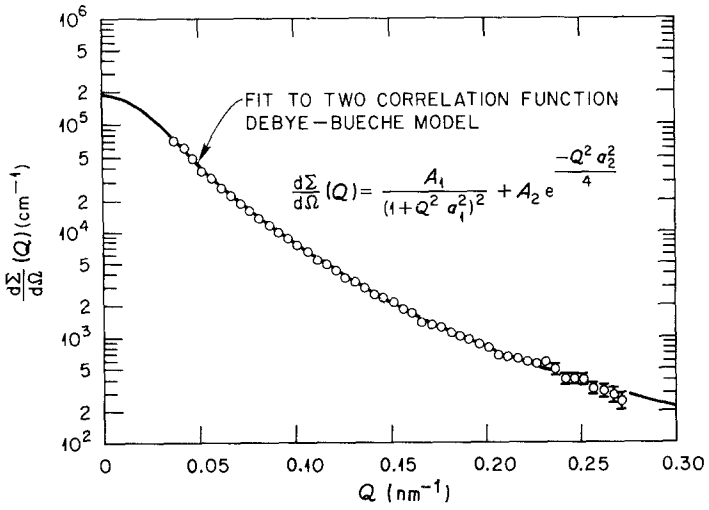

Figure 3 Coherent SANS cross-section from 34.8 vol % carbon black in polyethylene.

of the calculated intensities to the correlation lengths. The dimensions of the fitted correlation lengths are in the range 10 to 30 nm for a_1 and 50 to 80 nm for a_2.

Although the SAXS data can be fitted by the same method (Equation 5) the correlation lengths are different to those measured by SANS and fall in the range 12 to 15 nm for a_1 and 37–42.5 nm for a_2. This is illustrated in Fig. 5 which shows SANS and SAXS data for 34.8 vol % carbon. It may be seen that the SANS data measured in two different Q-ranges agree quite well, but the shape of the SAXS data is different, particularly at low Q. This indicates that the scattering cannot arise from a simple two-phase model consisting of carbon particles in a polyethylene matrix. If this were the case then the SAXS and SANS data could be superimposed by a simple multiplicative scale factor [19].

This discrepancy suggests that there are more than two phases involved in the scattering, and we believe that this arises from small voids at the surface of the carbon particles. This hypothesis is supported by the data given in Table II, which shows a small but consistent reduction in measured density against calculated density based upon a zero void assumption. The contribution to the scattering from the three phases may be estimated from Table V which shows the contrast factors for SAXS and SANS. Because of the near equivalence of the scattering length densities (SLD) of voids and polyethylene, the SANS experiment may be treated to a good approximation by a two-phase model, because the polyethylene is virtually "invisible" to neutrons and is indistinguishable from voids. This is because the voids have virtually no SANS contrast with the polyethylene matrix due to the cancellation between the coherent neutron scattering lengths of carbon and hydrogen. On the other hand, voids would have a large SAXS contrast with both carbon and polyethylene due to the large electron density difference involved (Table V). SANS can therefore give an accurate description of the morphology of the carbon particles as indicated by the good agreement of the SANS cross-sections with the simple two-phase theory. The SAXS patterns, on the other hand, are sensitive to the morphology of all three phases and therefore do not have the same shape as the SANS data (Fig. 5).

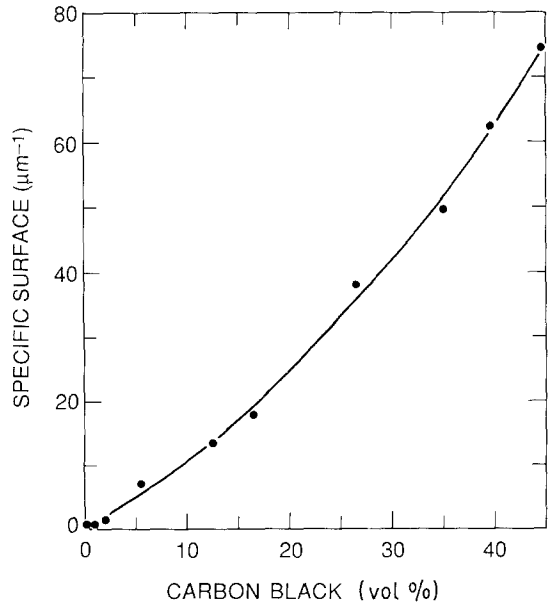

Figure 4 Concentration dependence of specific surface for carbon black–polyethylene blends.

The scattering from three-phase composite systems consisting of polymer, filler and voids has been discussed by Wu [25]. Using the subscripts 1, 2, and 3 to designate the filler (carbon) particles, voids and polymer matrix, respectively, the SANS invariant integral is given by

$$I = \int_0^\infty Q^2 \frac{d\Sigma}{d\Omega} dQ$$
$$= 2\pi^2 [(\varrho_1 - \varrho_2)^2 \phi_1 \phi_2 + (\varrho_2 - \varrho_3)^3 \phi_2 \phi_3 + (\varrho_3 - \varrho_1) \phi_3 \phi_1] \quad (14)$$

TABLE IV Comparison of measured and calculated values of absolute SANS cross section at $Q = 0$

ϕ (%)	$\frac{d\Sigma}{d\Omega}(0)$ (10^3 cm^{-1})	
	Measured	Calculated from Equation 13
44.5	97.7	76.9
39.5	159	118
34.8	177	166
26.3	237	200
16.5	317	380
12.4	247	345
5.6	178	182
1.08	14.1	50.0
0.53	32.2	24.4
0.27	8.0	10.9

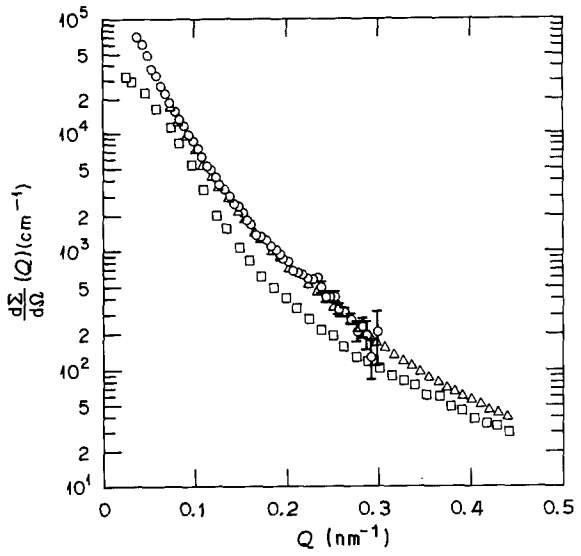

Figure 5 $(d\Sigma/d\Omega)(Q)$ for SANS and SAXS data from 34.8 vol % carbon in polyethylene. (○) SANS from 18.9 m data, (△) SANS from 10 m data, (□) SAXS from 5 m data.

where ϕ_i is the volume fraction and ϱ_i is the scattering length density of the ith phase. The SAXS invariant is given by a similar expression in which the SLD is replaced by the electron density times the Thompson scattering factor (0.282×10^{-12} cm). If there are no voids present in the system ($\phi_2 = 0$), the SAXS invariant may be calculated from Equation 14, the known electron densities (Table V) and volume fractions. For the sample containing 34.8% carbon the measured and calculated values for I_{SAXS} are $(0.013 \mp 0.03) \times 10^{24}\,cm^{-4}$ and $0.016 \times 10^{24}\,cm^{-4}$, respectively. The measured invariant for SANS is $(0.018 \mp 0.03) \times 10^{24}\,cm^{-4}$ compared to a value of $0.016 \times 10^{24}\,cm^{-4}$ calculated on the assumption that $\phi_2 = 0$. This indicates that the volume fraction of voids is small and cannot be determined by measurements of the SAXS and SANS invariants. This is consistent with density measurements which indicate that $\phi_2 < 0.01$.

The fact that the SAXS and SANS intensities at low Q cannot be scaled by a single multiplicative factor indicates that structural analyses based on only one type of measurement can easily give rise to misleading

TABLE V Contrast factors for SANS and SANS in carbon black-filled polyethylenes

	Electron density $EL(10^{-23}\,cm^{-3})$ (SAXS)	Scattering length density $(10^{-10}\,cm^{-2})$ (SANS)
Carbon black	5.40	5.98
Polyethylene	3.26	−0.34
Void	0	0

conclusions. If our hypothesis of void scattering is correct, then SAXS analysis is particularly vulnerable to this artefact. In this particular investigation, SANS gives a much better picture of the morphology of the carbon particles because of the near equivalence of the scattering power of voids and the polymer matrix. In any eventuality, the combination of SAXS and SANS measurements provides a good check on the validity of the two-phase assumption.

Measurements at higher values of Q are sensitive to fluctuations in scattering power over smaller length scales, and at a given value of Q the experiment probes a length scale of order $2\pi Q^{-1}$. Scattering from porous or particulate media can often be expressed as a power law over a wide range of Q [17, 26, 27] and such behaviour is often associated with fractal systems showing self similarity over different length scales. For a fractal analysis to be valid, the data should fit a single exponent $n(I \sim Q^{-n})$ over a wide Q-range. The simple Debye–Bueche model ($f = 1$ in Equations 3 and 4) gives the Porod exponent ($n = 4$), though the actual measured exponents (Table VI) fall in the ranges 3.0 to 3.7 (SANS) and 3.2 to 3.4 (SAXS). Thus the simple Debye–Bueche or Porod analyses previously used in the analysis of particle-reinforced polymers [5–7] do not give an adequate description of the scattering from the materials studied in this work. Fig. 6 shows SAXS and SANS data for a typical sample and indicates the ranges over which the exponents were evaluated. The differences introduced by using two different fitting ranges for SANS ($0.13 < Q < 0.25\,nm^{-1}$) and SAXS ($0.13 < Q < 1\,nm^{-1}$) were investigated by fitting some SAXS data sets over the same range as SANS. The results are given in Table VI

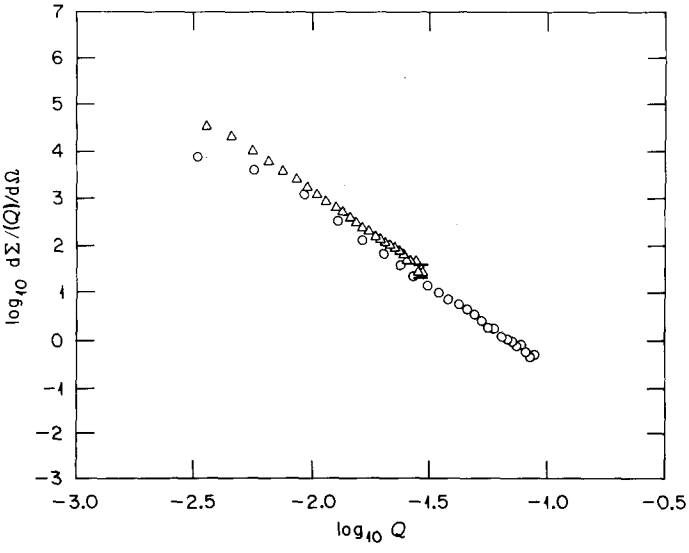

Figure 6 Log $(d\Sigma/d\Omega)$ (Q) plotted against log Q for 5.6 vol % carbon black in polyethylene. (△) SANS, (○) SAXS.

TABLE VI Power law exponents for SAXS and SANS

ϕ(%)	SANS ($0.13 < Q < 0.25\,nm^{-1}$)	SAXS ($0.13 < Q < 0.25\,nm^{-1}$)	SAXS ($0.13 < Q < 1\,nm^{-1}$)
44.5	2.98	3.27	3.23
39.5	3.18		3.26
34.8	3.39	3.38	3.29
26.3	3.55	3.22, 3.38	3.32, 3.32
16.5	3.65		3.30
12.4	3.63		3.36
5.6	3.57	3.43	3.38
1.08	3.68		3.38

and show that the differences in n introduced by fitting over two ranges (i.e. ~ 0.04) are not sufficient to explain the systematic discrepancies between the SAXS and SANS exponents. The obvious explanation for this discrepancy is the presence of voids caused by incomplete wetting or bonding of the carbon particles to the filler during mixing. This analysis therefore suggests that the exponents derived fron SANS analyses may be used to characterize the carbon particles due to the fact that the neutron experiments are insensitive to voids. Exponents of order $n = 3.5$ have been observed for certain types of carbon black and can be explained in terms of scattering from fractally rough pore surfaces or in terms of a power law distribution of particle sizes [27].

Small-angle scattering is clearly a powerful technique in the study of filled systems, being nondestructive and allowing experiments to be carried on bulk samples. This work has shown that scattering data from concentrated two-phase (and three-phase) systems can be successfully modelled theoretically. Future work will attempt to correlate the scattering parameters with physical and electrical properties of such systems.

Acknowledgements

The authors thank Mark Wartenberg for help in sample preparation and for helpful discussions. The research was sponsored in part by Raychem Corporation, in part by the National Science Foundation under grant RDM-8616912, and in part by the Division of Materials Science, US Department of Energy, under contract DE-AC05-840R-21400 with Martin Marietta Energy Systems, Inc.

References

1. A. I. MEDALIA, in "Carbon Black–Polymer Composites", edited by E. K. Sichel (Marcel Dekker, New York, 1982).
2. J. H. BACHMAN, F. W. SELLERS, M. P. WAGNER and R. F. WOLF, *Rubb. Chem. Technol.* **32** (1950) 1286.
3. A. I. MEDALIA and F. A. HECKMAN, *Carbon* **7** (1969) 567.
4. D. RIVIN, *Rubb. Chem. Technol.* **32** (1959) 1286.
5. D. S. BROWN, F. P. WARNER and R. E. WETTON, *Polymer* **13** (1972) 575.
6. T. P. RUSSELL, *J. Polym. Sci. Polym. Phys. Edn* **22** (1984) 1105.
7. R. J. YOUNG, D. H. A. AL-KUDHAIRY and A. G. THOMAS, *J. Mater. Sci.* **21** (1986) 1211.
8. S. MORRIS, G. D. WIGNALL, N. FARRAR and P. SONI, NCSASR Reports of Measurements, 1981–1982, Oak Ridge National Laboratory, October 1982.
9. R. W. HENDRICKS, *J. Appl. Crystallogr.* **11** (1978) 15.
10. G. D. WIGNALL, W. E. MUNSIL and C. J. PINGS, *ibid.* **11** (1978) 44.
11. G. D. WIGNALL, D. K. CHRISTEN and V. RAMAKRISHNAN, *ibid.* **21** (1988) 438.
12. W. C. KOEHLER, *Physica* **137B** (1986) 320.
13. G. POROD, *Kolloid Z.* **124** (1951) 83.
14. *Idem, ibid.* **125** (1952) 51.
15. P. DEBYE and A. BUECHE, *J. Appl. Phys.* **20** (1949) 518.
16. P. DEBYE, H. R. ANDERSON and H. BRUMBERGER, *ibid.* **28** (1957) 679.
17. D. W. SCHAEFER, "Materials Research Society Symposium Proceedings", Vol. 79, edited by G. D. Wignall, B. Crist, T. P. Russell and E. L. Thomas (Pittsburgh, 1987) p. 47.
18. G. D. WIGNALL and F. S. BATES, *J. Appl. Crystallogr.* **20** (1987) 28.
19. T. P. RUSSELL, J. S. LIN, S. SPOONER and G. D. WIGNALL, *ibid.* **21** (1988) 629.
20. A. M. FERNANDEZ, G. D. WIGNALL and L. H. SPERLING, *Adv. Chem.* **211** (1986) 10.
21. G. W. LONGMAN, G. D. WIGNALL, H. HEMMING and J. V. DAWKINS, *Colloid Polym. Sci* **252** (1974) 298.
22. D. J. BLUNDELL, G. W. LONGMAN, G. D. WIGNALL and M. J. BOWDEN, *Polymer* **15** (1974) 33.
23. M. MORITANI, T. INOUE, M. MOTEGI and H. KAWAI, *Macromol.* **33** (1970) 433.
24. H. K. YUEN and J. B. KISSINGER, *ibid.* **7** (1974) 329.
25. W. WU, *Polymer* **23** (1982) 1907.
26. P. Z. WONG, J. HOWARD and J. S. LIN, *Phys. Rev. Lett.* **57** (1986) 637.
27. D. W. SCHAEFER and A. J. HURD, in "Proceedings of the Symposium on the Chemistry and Physics of Composite Media", edited by M. Tomkeiwicz and P. N. Sen (Electrochemical Society, 1986) p. 85.

Received 27 September 1988
and accepted 27 February 1989